

## Control method of one-branch controlled three-phase rectifier with no rotor position detection

**Streszczenie.** Artykuł przedstawia metodę sterowania prostownika trójfazowego z jedną gałęzią sterowaną współpracującego z generatorem z magnesami trwałymi (PM), dzięki której nie jest wymagana informacja o położeniu wirnika (NRP) generatora. Połączenie prostej metody sterowania z niskimi kosztami budowy tego typu prostownika może być interesującym, niezawodnym rozwiązaniem dla turbin wiatrowych małej mocy lub alternatorów samochodowych. Omówiono zależności matematyczne opisujące moc wyjściową prostownika. Zweryfikowano eksperymentalnie wpływ klasycznej i nowej metody sterowania na sprawność prostownika.

**Abstract.** This paper presents control strategy of the one-branch controlled three-phase rectifier cooperating with permanent magnet (PM) generator which allows for operation with no rotor position detection (NRP) of the generator. Combination of a proposed simplified control algorithm and low-cost rectifier can be an interesting reliable solution for permanent-magnet (PM) small-scale wind turbines or automotive alternators. Mathematical relationships for the rectifiers' output power are discussed. The influence of new and classic control strategy on efficiency was experimentally verified. *Metoda sterowania prostownika trójfazowego z jedną gałęzią sterowaną współpracującego z generatorem z magnesami trwałymi*

**Słowa kluczowe:** przekształtnik AC/DC do współpracy z generatorem PM; prostownik sterowany; trójfazowy przekształtnik z jedną gałęzią sterowaną.

**Keywords:** AC/DC converter for PM generator; controlled rectifier; one-branch controlled three phase rectifier.

### Introduction

In recent years environmental pollution and the energy crisis are rising globally. In this context, the high efficiency of electric devices is a desirable means to reduce power consumption. An electric motor is the main element that converts mechanical energy into an electrical energy and does the reverse conversion. Nowadays PM motors become more and more popular because of high efficiency, dynamic capability, high energy density and reliability. Therefore, they are commonly applied in military, industrial and domestic equipment. Modern PM motors usually cooperate with different type of power converters to obtain high efficiency across a wide range of electromechanical characteristics [1-8]. The full-bridge controlled converter is a widely used solution for PM motors which associate two other phases with the highest instantaneous value of back EMF voltages [9]. This makes it possible to fully assemble the electromagnetic energy of the motor. In standard solutions, the controller reads the Hall sensor signals and decides the appropriate phase to be commutated [10], [11]. The paper concentrates on converters that allow for the regenerative braking of PM motors. Therefore, in the next part of the paper, PM motor is called PM generator and converter is called rectifier. Different kinds of rectifiers are widely used in small-scale wind-turbines and automotive alternators [12]. An often-omitted criterion for this kind of systems is cost and reliability. The one-branch controlled three-phase rectifier shown in Fig.1 fulfills the above demands. The switching strategy proposed in this paper is different from the one described in [13] as no rotor position sensing is needed. Fig.2 shows back-EMF voltages of the PM generator, hall sensor signals, transistor control signals for classic-sensored and NRP control.

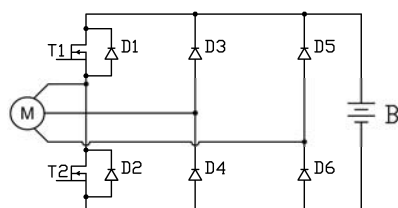


Fig.1. One-branch controlled three-phase rectifier

### Operational principles

The operational principle is similar to that of the DC/DC boost converter. The rectifier has two operational stages. At the first stage rotor kinetic energy is converted into electric energy and stored in magnetic field of stator windings. At the second stage the stored electric energy flows to the battery.

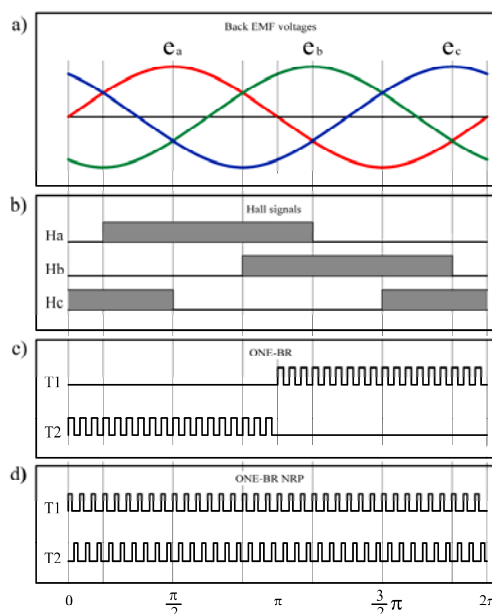


Fig.2. a) back-EMF voltages, b) hall sensor signals, c) transistor control signals for classic-sensored control, d) NRP control

Fig.3 shows the three-phase back-EMF voltages and the control signals for  $T1$ ,  $T2$  transistors. Consider the interval angle from 0 to  $\pi/2$ . When the phase voltage  $e_a$  is greater than zero transistor  $T2$  is turned on - rotor kinetic energy is converted into electric energy and stored in the magnetic field of stator windings as shown in Fig.3.a. The current circuit is completed by transistor  $T2$  associated with the highest voltage  $e_a$  and diode  $D4$  associated with lowest voltage  $e_b$ . When transistor  $T2$  is turned off battery is charging. It can be noticed that the battery is charged partly through by transistor  $T1$  and diode  $D1$ , Fig.3.c.

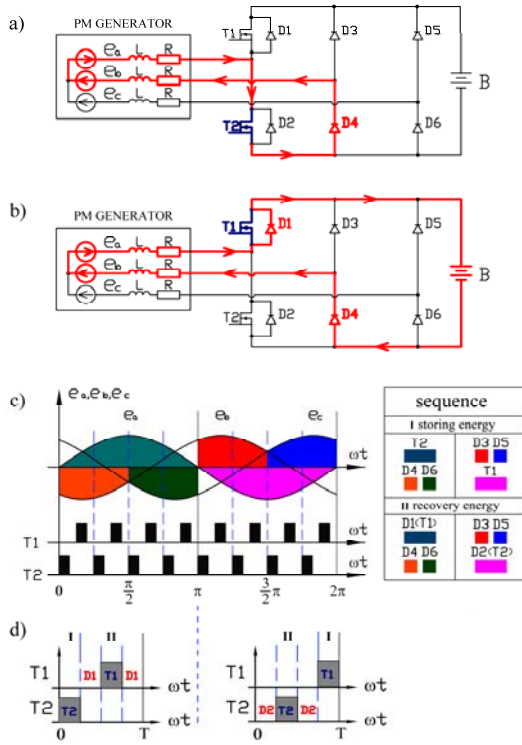


Fig.3. Current flow for angle range  $0-\pi/2$  a) storing energy, b) recovery energy, c) back EMF voltages of the generator, d) switching sequence

Considering Fig.3.d it can be observed that control signals of transistors are symmetrical under a half of the modulation period  $T/2$ . High ( $T1$ ) and low ( $T2$ ) side voltage transistors associated with phase  $a$  properly participate in storing "I" and recovery "II" energy process, independently of the instantaneous value of the generators back EMF voltage  $e_a$ . This allows for NRP operation of the one-branch controlled three-phase rectifier in the range of duty cycles from 0% up to 50% (decreased by dead time).

### Simulation results

Simulation studies of the one-branch controlled rectifier, NRP operation, were carried out under the following assumptions: the transistor is an ideal switch, diode in the on state is modeled by constant-voltage  $U_f$  and in the off state by infinite resistance, all passive elements are linear, time is invariant, back-EMF voltages have ideal sinusoidal shape. The mathematical model based on the continuity of the current flowing through the inductances and volt-second balance was created [11], [14]. The figures Fig.4.a and Fig.4.b show the equivalent circuits for storing/recovery energy process.

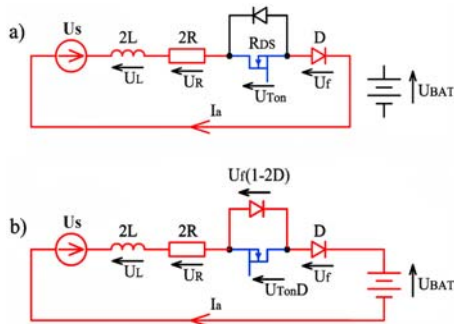


Fig.4. Equivalent circuits for a) storing energy, b) recovery energy from the inductances

According to the volt second balance principle we can conclude

$$(1) \quad \frac{1}{L} \int_0^T u_L(t) dt = U_L(t_{on}) + U_L(t_{off}) = 0$$

where:  $U_L(t_{on})$  and  $U_L(t_{off})$  are the average inductor voltages. The voltage generator  $U_S$  is equal to average interphase voltage and can be expressed as

$$(2) \quad \int_0^{\pi/2} (e_a(t) - e_b(t)) d\omega t = \frac{3\sqrt{2} - \sqrt{6}}{\pi} U_{RMS} = a U_{RMS} = a k \omega$$

Inductor average voltages can be expressed as

$$(3) \quad U_L(t_{on}) = DT(ak\omega - I_a(2R + R_{DS}) - U_f)$$

$$(4) \quad U_L(t_{off}) = (1-D)T(ak\omega - I_a(R_B + 2R + DR_{DS}) - U_{BAT} - (1-2D)U_f)$$

where:  $D$  - PWM duty cycle,  $T$  - period time,  $I_a$  - average armature current,  $R_B$  - battery internal resistance,  $R$  - generator phase resistance,  $R_{DS}$  - static drain-to-source on-resistance of the transistor,  $U_{BAT}$  - battery voltage,  $U_f$  - diode forward voltage.

Putting (3) and (4) into (1), the average armature current of the generator can be determined. Since battery charging takes place during  $(1-D)$  of the period time, the formula for the output power of the rectifier  $P_{OUT}$  can be obtained.

$$(5) \quad P_{out} = (1-D)U_{BAT}I_a$$

$$(6) \quad I_a = \frac{ak\omega - (2D^2 - 2D + 1)U_f - (1-D)U_{BAT}}{2R + R_B(1-D) + R_{DS}(2D - D^2)}$$

Output power of the rectifier depends on the relation of the battery voltage and the total RMS phase voltage of the generator and the PWM duty cycle. Simulation results for the NRP operation of the One-Branch rectifier are presented below.

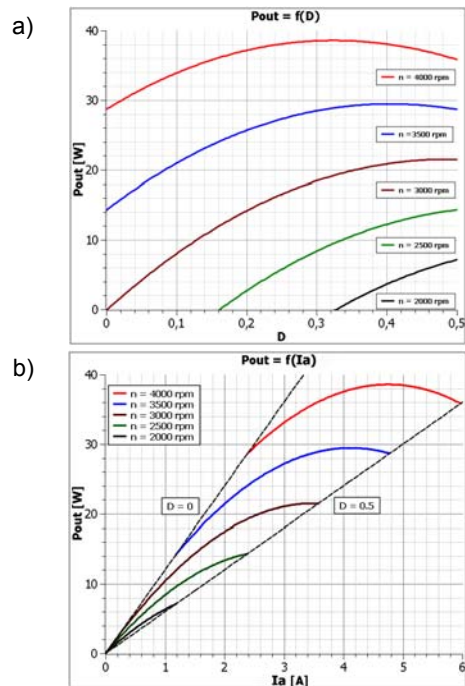


Fig.5. Output power  $P_{OUT}$  for five generator speeds in the function of a) duty cycle, b) average generator current

The Fig.5.a presents output power of One-Branch three phase rectifier for NRP operation for several rotational speeds of the generator. It can be observed that maximum of the output power can be obtained with lower duty cycles for increasing generator speed. For 3000 rpm this maximum occurs close to 50% of the duty cycle. At this speed the maximum instantaneous phase voltage is equal to the battery voltage. This allows for full control of rectifier output power and average generator current ranging from 0 A as shown in Fig.5.b For higher speeds the uncontrolled diode conduction occurs.

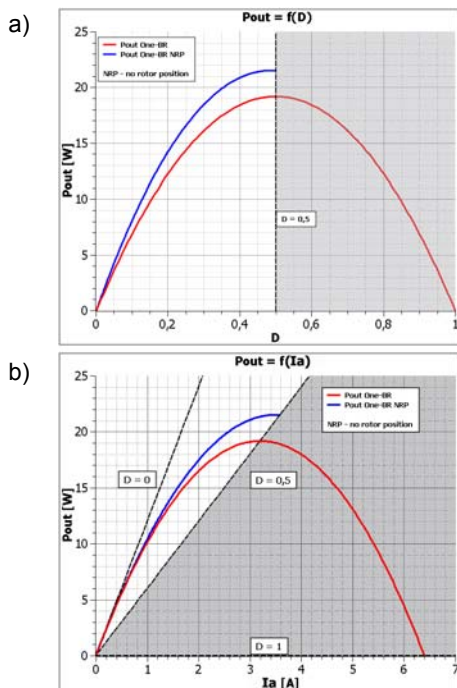


Fig.6. Output power  $P_{OUT}$  for 3000 rpm in the function of a) duty cycle, b) average generator current

Considering Fig.6.a and Fig.6.b it can be concluded that NRP operation allows to get larger maximum output power than sensed control. As apparent from the Eq.3, this differences are caused by voltage drops occurring during transistor and diode conduction process. These losses depend on the duty cycle and the battery voltage. Simulation conditions are presented in Tab.1.

Table 1 Simulation parameters

R	0.87	$\Omega$	generator phase resistance
$R_{DS}$	0.023	$\Omega$	static drain-to-source on-resistance of the transistor
$R_B$	0.02	$\Omega$	battery internal resistance
$U_{BAT}$	12	V	battery voltage
$U_f$	0.7	V	diode forward voltage
D	0-1	-	PWM duty cycle
k	0.05	-	voltage constant
n	1000-4000	rpm	generator speed

### Experimental results

Experimental studies for NRP and sensed operation were carried out. The experimental set-up is shown in [12]. It consists of one-branch controlled three-phase rectifier composed of IRFP90N20D MOSFET transistors and HFA15PB60 diodes, Parvalux PBL60-78 PM generator and the Yokogawa Power Analyzer WT 1600. An exemplary experimental plots of the output voltage and phase currents of the generator are shown in Fig.7.

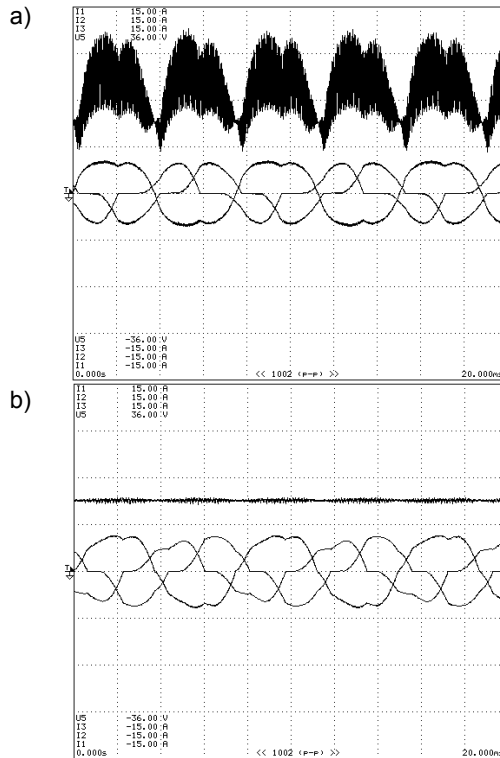


Fig.7. Output voltage and phase currents for 4000 rpm (a) resistive load, (b) lead-acid battery load

### A. Output power characteristics

Fig.8 shows output power of one-branch controlled three phase rectifier in the function of duty cycle and generator phase RMS current for 3000 rpm.

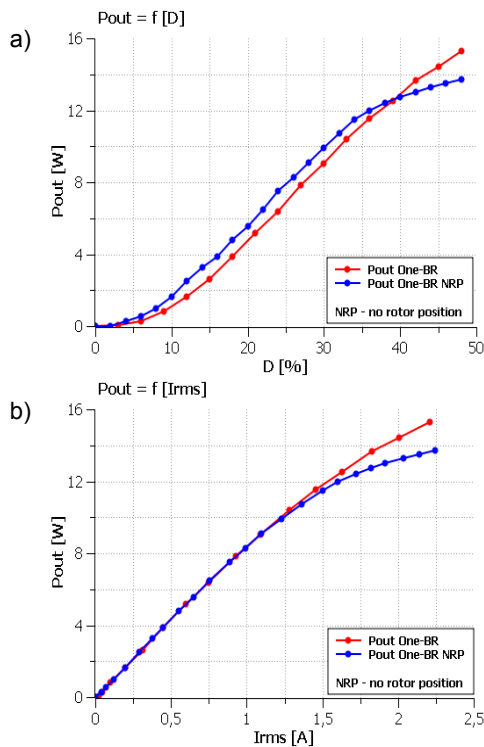


Fig.8. Output power  $P_{OUT}$  for 3000 rpm in the function of (a) duty cycle, (b) generator phase RMS current

Considering Fig.8 we can conclude that in the range of 10 ÷ 35% of the duty cycles NRP operation allows us to

achieve the output power greater by about 9% than the sensed operation. It can be observed that above 40% of the duty cycle output power for the NRP algorithm decreases. It is caused by the dead time which reduces the useful range of the duty cycles.

### B. Efficiency characteristics

The efficiency of the one-branch controlled three-phase rectifier in the function of PWM duty cycle D and generator phase RMS current is shown in Fig.9.

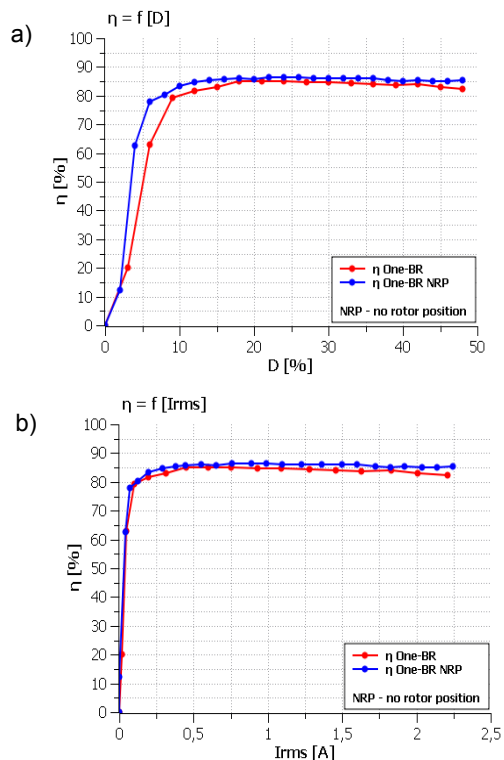


Fig.9. Efficiency for 3000 rpm in the function of a) duty cycle, b) generator phase RMS current

As Fig.9.b shows that the efficiency for NRP operation reaches about 87% and for sensed one 85%. The difference is caused by different conduction losses for each control method. It can be noticed that both efficiencies are maintained at a constant level in the range of  $0.25 \div 2.5A$ .

### Conclusions

The novel control method for the one-branch controlled three-phase rectifier presented in the paper makes it possible to conduct NRP operation. The efficiency achieved is higher than the one obtained for sensed operation in a wide range of useful duty cycle. This is result of synchronous rectification of the MOSFET transistor that takes over a part of diode current in the regeneration period (Fig.4b MOSFET drop-voltage is considerably smaller than diode forward voltage). To achieve full control of the output power the higher speed of the generator is required as compared with the sensed operation. It is caused by a 50% limitation of usable range of the duty cycle. Due to dynamic changes of the generator speed, the

implementation of the transmissions can be necessary. This is the main disadvantage of the proposed control method. Also dead-time should be as short as possible to achieve duty cycle range regulation close to 50 %. NRP control can be successfully used in small-power low-cost wind generators.

**Authors:** dr hab. inż. Sławomir Karyś, Politechnika Świętokrzyska, Zakład Energoelektroniki, Maszyn i Napędów Elektrycznych, ul. al. Tysiąclecia Państwa Polskiego 7, 25-314 Kielce, E-mail: enesk@tu.kielce.pl; mgr inż. Paweł Stawczyk, Politechnika Świętokrzyska, Zakład Energoelektroniki, Maszyn i Napędów Elektrycznych, ul. al. Tysiąclecia Państwa Polskiego 7, 25-314 Kielce, E-mail: pstawczyk@tu.kielce.pl

### REFERENCES

- [1] Singh B, Singh S, State of the Art on Permanent Magnet Brushless DC Motor Drives, *Journal of Power Electronics*, Vol. 9, No. 1, January (2009)
- [2] Biskup T, Bodora A, Domoracki A, A reconfigurable structure electronic commutator for a dual BLDC motor EV drive, *Bull. Pol. Ac.: Tech.* 60 (4), 769-778 (2012)
- [3] Fan S, Lim T, Zhang H, Finney S, Williams B, Design and Control of Wind Energy Conversion System Based On Resonant DC/DC Converter, *IET Conference on Renewable Power Generation* (2011)
- [4] Shang H, Tolbert L. M, Efficiency Impact of Silicon Carbide Power Electronics for Modern Wind Turbine Full Scale Frequency Converter, *IEEE Transactions on Industrial Electronics*, Vol. 58, Issue: 1, 21-28 Jan. (2011)
- [5] Yang G, Zhu Y, Application of a Matrix Converter for PMSG Wind Turbine Generation System, 2nd *IEEE International Symposium on Power Electronics for Distributed Generation Systems*, 185-189 (2010)
- [6] Yogesh Murthy N, A Review on power electronics application on wind turbines, *International Journal of Research in Engineering and Technology*, Volume: 02 Issue: 11 Nov. (2013)
- [7] Khater F, Shaltout A, Omar A, Control of direct-driven PMSG for wind energy, *18th International Conference on Systems (part of CSCC '14)*, 455-461 (2014)
- [8] Mazgaj W, Szular Z, Węgiel T, Sobczyk T, Small Hydropower Plant with variable speed PM generator, *Przegląd Elektrotechniczny*, R. 87 NR 5, 282-287 (2011)
- [9] Xu Y, Tang Y, Zhu J, Zou J, Ma C, Control of a BLDC Motor for Electromechanical Actuator, *Conference: Electrical Machines and Systems ICEMS*, 3266-3269 (2008)
- [10] Zhang K., Electric Braking Performance Analysis of PMSM for Electric Vehicle Applications, *2011 International Conference on Electronic & mechanical Engineering and Information Technology*, 2596-2599 (2011)
- [11] Chen C, Chi W, Cheng M, Regenerative Braking Control for Light Electric Vehicles, *IEEE PEDS*, 5-8 December Singapore, 631-636 (2011)
- [12] Pathmanathan M, Tang C, Soong W.L, Ertugrul N, Comparison of Power Converters for Small-Scale Wind Turbine Operation, *Australasian Universities Power Engineering Conference*, 1-6 (2008)
- [13] Stawczyk P, Karyś S, Three-Phase One-Branch Controlled Bridge Rectifier for Permanent Magnet ac Synchronous Generator, *CPE Powereng, Bydgoszcz*, 450-454 (2016).
- [14] Jiaqun X, Jie. J, Haotian C, A Controlled Rectification Method for Automotive Brushless DC Generator with Ultracapacitor Energy Storage, *16th International Power Electronics and motion Control Conference Exposition, Antalya, Turkey* 21-24 Sept, 168-173 (2014)